



Cite this: DOI: 10.1039/c4nr06237j

Received 23rd October 2014,  
Accepted 1st December 2014

DOI: 10.1039/c4nr06237j

www.rsc.org/nanoscale

## Controllable fabrication of ultrafine oblique organic nanowire arrays and their application in energy harvesting

Lu Zhang,<sup>†a</sup> Li Cheng,<sup>†a</sup> Suo Bai,<sup>a,b</sup> Chen Su,<sup>a</sup> Xiaobo Chen<sup>a</sup> and Yong Qin<sup>\*a,b</sup>

Ultrafine organic nanowire arrays (ONWAs) with a controlled direction were successfully fabricated by a novel one-step Faraday cage assisted plasma etching method. The mechanism of formation of nanowire arrays is proposed; the obliquity and aspect ratio can be accurately controlled from approximately 0° to 90° via adjusting the angle of the sample and the etching time, respectively. In addition, the ONWAs were further utilized to improve the output of the triboelectric nanogenerator (TENG). Compared with the output of TENG composed of vertical ONWAs, the open-circuit voltage, short-circuit current and inductive charges were improved by 73%, 150% and 98%, respectively. This research provides a convenient and practical method to fabricate ONWAs with various obliquities on different materials, which can be used for energy harvesting.

### Introduction

Along with the rapid development of nanotechnologies in recent years, organic nanowires (NWs) as promising building blocks for fabricating smart nanodevices have been extensively applied in organic light-emitting diodes,<sup>1</sup> organic solar cells,<sup>2</sup> field effect transistors,<sup>3</sup> sensors,<sup>4,5</sup> and supercapacitors<sup>6</sup> due to their excellent physical properties and ingenious surface features.<sup>7,8</sup> Organic nanowire arrays (ONWAs) with controlled orientation have shown excellent performance in many aspects in contrast to the random and misaligned structures.<sup>9</sup> Their unique anisotropic properties have been widely applied in microfluidic devices,<sup>10</sup> self-cleaning surfaces,<sup>11</sup> object transport,<sup>12</sup> dry adhesives<sup>13</sup> and reflection gating.<sup>14</sup> Broadly speaking, ONWAs can be divided into three types: vertical ONWAs, horizontal ONWAs and oblique ONWAs. In previous work, vertical ONWAs have been fabricated through different conven-

tional approaches including block copolymer self-assembly,<sup>15</sup> plasma etching<sup>16,17</sup> and replica molding techniques.<sup>18–21</sup> On the other hand, horizontal ONWAs have also been made *via* various methods such as template free deposition,<sup>22</sup> nano-imprint lithography<sup>23,24</sup> and wrinkling methods.<sup>25</sup> Compared with the two types above, although a few approaches have been explored for fabricating oblique ONWAs, the fabrication of oblique ONWAs, especially the ultrafine ONWAs with a controllable direction, is still very difficult. For instance, conventional inclined lithography can be employed to fabricate well-defined oblique micropillars distributed uniformly<sup>26</sup> but the refraction and wavelength of incident light limit the angle of inclination and the aspect ratio (AR). In addition, although the mask-assisted low energy ion milling method can realize the obliquity of uniform ONWAs varying from 10° to 40°,<sup>12</sup> the variation range is small and its formation mechanism leads to its low AR. Furthermore, though the ONWAs fabricated by oblique angle polymerization can possess high AR,<sup>27,28</sup> the obliquity cannot be controlled easily and the density is too high to identify the profile of every NW. Hence, now it is a challenge and highly desirable to controllably fabricate high quality oblique ONWAs with high AR on a large scale.

In this paper, we reported a novel one-step Faraday cage assisted plasma etching method for the controllable fabrication of ultrafine oblique ONWAs with high AR on a large scale. Moreover, we studied the formation mechanism of the oblique ONWAs. In the fabrication process, the moving direction of ions was controlled by the Faraday cage and the ions bombarded on the samples obliquely. The obliquity of ONWAs can be accurately controlled by adjusting the slope of the samples from 0° to 90°, and the length of ONWAs can be simply controlled *via* adjusting the etching time. By using their anisotropic mechanical properties and high AR, the output performance of a triboelectric nanogenerator (TENG) composed of ONWAs was greatly improved. The experimental result shows that the open-circuit voltage of the TENG composed of oblique ONWAs (OTENG) was 73% larger than that of the TENG composed of vertical ONWAs (VTENG), and the short-circuit current is also 1.5 times larger.

<sup>a</sup>Institute of Nanoscience and Nanotechnology, School of Physical Science and Technology, Lanzhou University, Lanzhou, 730000, China.

E-mail: qinyong@lzu.edu.cn

<sup>b</sup>The Research Institute of Biomedical Nanotechnology, Lanzhou University, Lanzhou, 730000, China

<sup>†</sup>These authors contributed equally to this work.

## Results and discussion

The oblique ONWAs were fabricated by direct reactive ion etching (RIE) without nanopatterns or prefabricated masks. As Fig. 1a shows, a cleaning polymer film was put obliquely on the bottom electrode of the RIE machine with an angle  $\alpha$  with respect to the electrode, and a Faraday cage consisting of a Cu grid top plane and Cu sidewall was covered over the film. The ONWAs were then formed after etching the polymer film under certain experimental conditions (details of the fabrication process are shown in the Experimental section). Fig. 1b shows a side view scanning electron microscopy (SEM) image of the fabricated oblique polyethylene terephthalate (PET) NW array after 70 minute etching. It can be seen that the NWs of about 30 nm in diameter and 2.3  $\mu\text{m}$  in length (aspect ratio = 76) distributed uniformly on the PET film, and the angle  $\theta$  between the nanowires and the PET film surface is about  $70^\circ$ , which is the coangle of the angle  $\alpha$ . Fig. 1c shows the Fourier transform infrared (FTIR) spectra of an untreated PET film and PET NWs fabricated by this method. There is no obvious difference between the two spectra, indicating that the ONWAs have the same chemical composition as the PET film. Hence, ultrafine ONWAs with a controlled direction can be *in situ* fabricated from a polymer sheet and have the same composition as the substrate.

In previous work, surface roughness or initial bumps formed on the polymer surface are explained as the reasons for the formation of ONWAs fabricated by plasma etching.<sup>17,29</sup> In this work, we propose a new mechanism for the formation of ONWAs based on experimental results. As shown in Fig. 2a, the fabrication process can be divided into two stages. First, a part of ions bombarded on the surfaces of the steel electrode and Cu grid during the accelerating path, which led to metal particles such as Cu, Fe, Cr, Mn and Zn sputtering off and depositing on the polymer surface. Meanwhile, a part of the

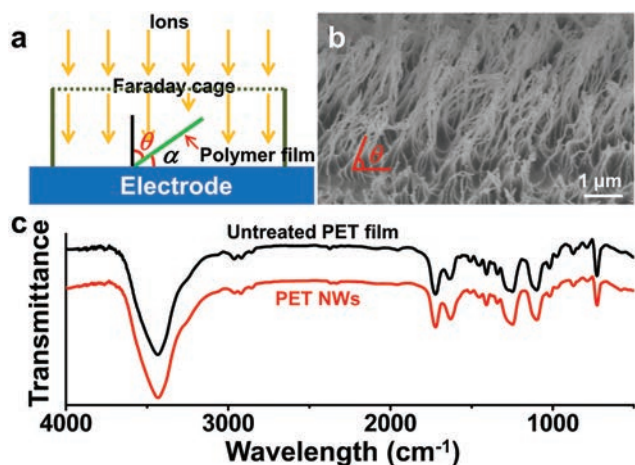


**Fig. 1** Fabrication schematic of the oblique ONWAs. (a) Schematic diagram of the fabrication equipment. (b) Side view of the SEM image of oblique PET NW arrays with the angle  $\theta$  of  $70^\circ$ . (c) FTIR spectra of the untreated PET film and PET NWs taken from PET NW arrays.

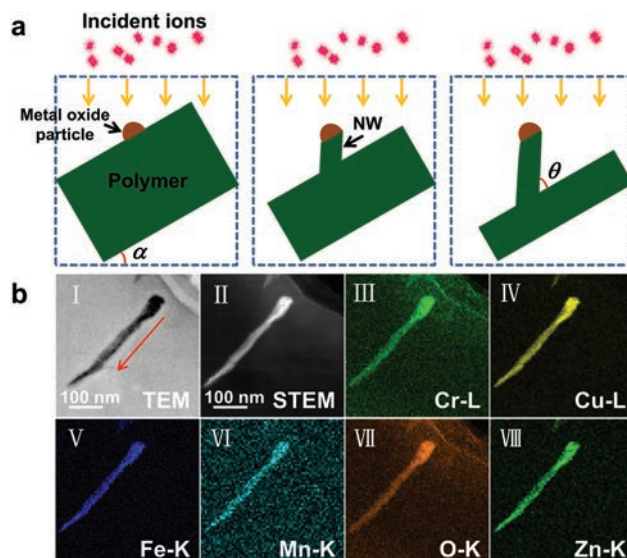


**Fig. 2** Formation mechanism of the oblique ONWAs. (a) Schematic image of the fabrication process. (b) BFTEM image (I), STEM image (II), and EDX mapping images (III–VIII) of a single PET NW taken from the PET NW array. The red arrow represents the orientation of the NW from the top to the bottom.

metal particles were oxidized under an oxygen atmosphere, and then the metal or metal oxide particles formed a mask on the surface and prevented the below polymer film from etching. Second, the ions passed through the Faraday cage and bombarded on the polymer with an angle  $\theta$  with respect to the film surface. During the fabrication process, the Faraday cage can control the moving direction of ions and further control the direction of the ONWAs *in situ* appearing on the film with the following mechanism. When a Faraday cage is employed under a plasma atmosphere a plasma sheath forms on the exterior surface of the Faraday cage, which leads to zero electric field inside the cage. Therefore, the ions can be accelerated in the electric field and pass through the hollows of the grid in the normal direction to the electrode plane. In contrast, without the Faraday cage, the plasma sheath forms on the surface of the substrate and the accelerated ions directly bombard on the substrate surface along its normal direction.<sup>13,30</sup> This implies that the angle of oblique etching can be easily controlled by adjusting the angle  $\alpha$  of the substrate covered by a Faraday cage. Therefore, the part of the polymer film without metal or metal oxide particles' protection was etched by the ions quickly, and oblique ONWAs with an angle  $\theta$  gradually formed on the surface of the film. In order to check the mechanism proposed above, we tested the distribution of elements on the surface of NWs. Fig. 2b shows the bright field transmission electron microscopy (BFTEM) image, scanning transmission electron microscopy (STEM) image and energy dispersive X-ray spectroscopy mapping (EDX mapping) images of Cu, Fe, Cr, Mn, Zn and O of a single PET NW. It is clear that all the elements of Cu, Fe, Cr, Mn, Zn and O have much higher concentration at the top of the NW and these metal elements are just the major composition of the steel



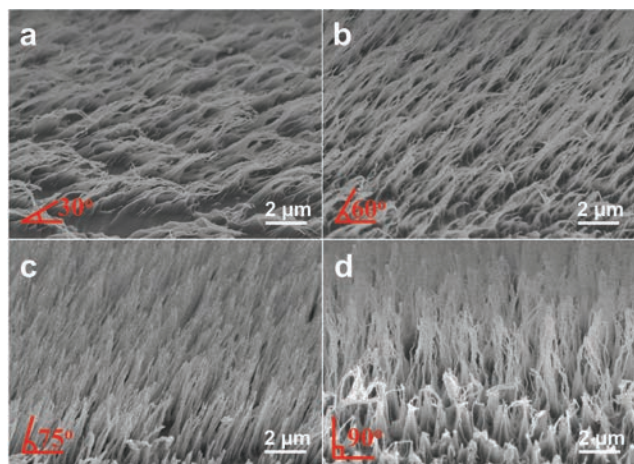


**Fig. 3** PET NW arrays with precisely controlled obliquity. (a–d) show the section view SEM images of PET NW arrays with angles of 30° (a), 60° (b), 70° (c) and 90° (d), respectively.

electrode and Cu grid, which further proves the above mechanism that the metal or metal oxide particles act as a mask in the etching process.

As the tilt angle of the polymer film can be accurately controlled in our experiment, the incident angle of ions with respect to the substrate could be controlled as well. Hence, the ONWAs with different obliquities on films can be fabricated by changing the tilt angle of the polymer film. In the experiment, we fabricated oblique PET NW arrays by placing the PET film at angles  $\alpha$  of 60°, 30°, 15° and 0°. The section view SEM images shown in Fig. 3 demonstrate that the PET ONWAs with different obliquities 30°, 60°, 75° and 90° have a similar size of about 2  $\mu\text{m}$  in length, 30 nm in diameter after 60 minute etching. This result indicates that the obliquity of the ONWAs can be accurately controlled in a wide range using this method. In addition, the size of ONWAs with different obliquities remains almost the same.

In addition, the ONWAs' length can be controlled easily by changing the etching time. Because of the metal or metal oxide mask existing on the top of the NWs to protect the polymer below in the whole fabrication process, the length of the NWs could grow continuously with the increasing etching time. Fig. 4a–f show the SEM images of PET NWs after 1, 5, 15, 30, 40 and 80 minutes of etching, respectively. Furthermore, a nearly linear relationship between the length of PET NWs and the etching time is observed as shown in Fig. 4g, which means that the oblique NW's length can be accurately controlled by simply adjusting the etching time.

A series of further experiments have been conducted to study whether the oblique ONWAs could be fabricated on any other polymers through this method. In the experiment, different substrates were located with an angle of 45° with respect to the electrode covered over by a Faraday cage. Fig. 5a–d show the SEM images of oblique ONWAs fabricated on a polyimide (Kapton) film, poly-*p*-phenylene terephthamide (Kevlar) fiber, carbon fiber and polypropylene (PP) fiber.

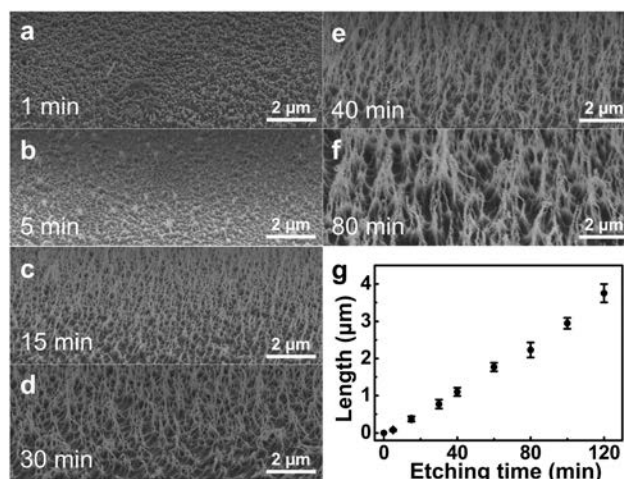


**Fig. 4** Length of PET NW arrays changes with different etching times. (a–f) show the section view SEM images of oblique PET NW arrays after 1 (a), 5 (b), 15 (c), 30 (d), 40 (e) and 80 (f) minutes of etching. (g) shows a nearly linear relationship between the etching time and the PET NWs' length.

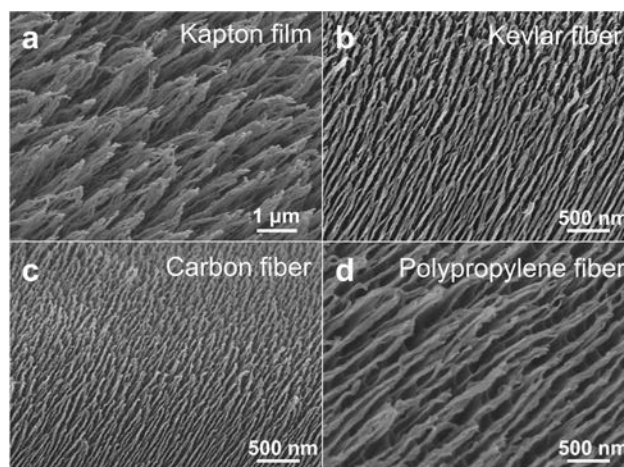


**Fig. 5** SEM images of oblique ONWAs fabricated on various substrates: (a) Kapton film, (b) Kevlar fiber, (c) carbon fiber, and (d) PP fiber.

The corresponding diameters are about 69, 42, 33 and 73 nm, respectively. This result reveals the wide versatility of this method. Using this novel one-step Faraday cage assisted plasma etching method, the oblique ONWAs of different materials can be fabricated on different kinds of substrates.

Oblique ONWAs have been widely employed in different areas due to their unique anisotropic properties. Nowadays, TENG is a new kind of device that can convert mechanical energy existing in the environment to electrical energy. The working principle of this TENG can be explained by the combination of the triboelectric effect and the electrostatic effect, which has been discussed clearly in previous work.<sup>31,32</sup> The TENG's performance is mainly determined by the materials' ability to gain or lose electrons and the structure of the device, and making micro/nanostructures is another important way to

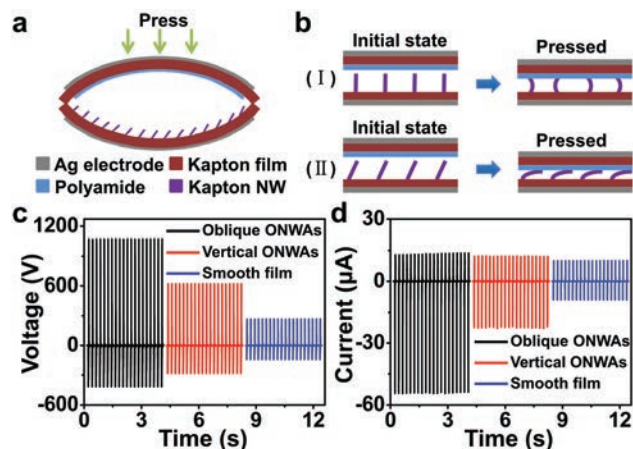


**Fig. 6** A TENG composed of oblique ONWAs. (a) Schematic image of an arch-shaped TENG. (b) Schematic diagram of the possible friction movements of the vertical NWs (I) and oblique NWs (II). When the two substrates are brought into contact, oblique NWs are easier to bend and slide on the surface of the Kapton film to enhance the friction. (c, d) Comparison of the open-circuit voltage (c) and the short-circuit current (d) of TENGs composed of oblique ONWAs, vertical ONWAs and a smooth film, respectively.

improve the TENG's performance.<sup>31–36</sup> With better designed nanostructures, the performance of TENG could be further improved. As shown in Fig. 6a, a typical arch-shaped TENG<sup>37</sup> was composed of two kinds of materials with different tendencies to gain or lose electrons. The materials selected here are a Kapton film with oblique ONWAs and a polyamide (nylon) film spin-coated on the Kapton film (details of the fabrication process are shown in the Experimental section). A previous study has reported that applying the vertical ONWAs on the TENG can improve the electric output of the device due to the enhanced surface roughness.<sup>31</sup> As the partial enlarged view of arch-shaped TENG is shown in Fig. 6b by replacing the vertical ONWAs with oblique ONWAs, it can be seen that the oblique NWs are easier to bend and slide on the surface of the Kapton film when the two substrates are brought into contact, which can enlarge the additional friction and produce much more triboelectric charges on the surface of electrodes.<sup>38</sup> Based on this assumption, the performance of the TENG is expected to be largely improved. Fig. 6c and d show that the open-circuit voltages of the OTENG, the VTENG and the TENG composed of a smooth film (STENG) are 1070 V, 620 V, and 265 V, and the short-circuit currents are 55  $\mu$ A, 22  $\mu$ A and 9  $\mu$ A, respectively. In addition, the corresponding inductive charges of these TENGs are 103 nC, 52 nC and 22 nC. Compared with the electric output of the STENG, the open-circuit voltage, short-circuit current and inductive charges of the VTENG increased by 134%, 144% and 136%, respectively. This enhanced performance was due to the improved surface roughness introduced by the vertical ONWAs, and this improvement can provide additional friction and generate more triboelectric charges.<sup>31</sup> Furthermore, compared with the electric output of the VTENG, the open-circuit voltage, short-circuit current and inductive charges of OTENG were improved

by 73%, 150% and 98%, respectively. The enhancement corresponded well to the assumption that the oblique NWs are easier to bend and slide on the surface of the Kapton film which leads to the enhancement of the additional friction and generates much more triboelectric charges. These results demonstrate that oblique ONWAs are effective in increasing the output energy of a TENG.

## Conclusions

In summary, we developed a novel one-step Faraday cage assisted plasma etching method for fabrication of ultrafine oblique ONWAs with the merit of high AR on a large scale and the precisely controlled obliquity and length. The formation of the ONWAs is due to the formation of a sputter-induced metal or metal oxidation mask and the mask-protected etching process. In addition, the oblique ONWAs were employed to improve the output of the TENG. Compared with the output of TENG composed of vertical ONWAs, the open-circuit voltage, short-circuit current and inductive charges were improved by 73%, 150% and 98%, respectively. This fabrication technique laid a solid foundation for the oblique ONWAs' potential applications including energy conversion, microelectronics, chemical and biological sensing.

## Experimental section

### Fabrication of oblique ONWAs on the surface of PET films

A PET film was first ultrasonically cleaned with acetone, ethanol and deionized water for 15 minutes successively, and then the film was blow-dried. Subsequently, the film was obliquely placed on the electrode of the RIE machine with an angle  $\alpha$  and then covered over by a Faraday cage consisting of a copper grid top plane and Cu sidewall; the top plane of the Faraday cage was placed parallel to the electrode. The diameter and the height of the Faraday cage employed in our experiment are 180 mm and 35 mm, respectively. After vacuumizing the chamber of the RIE machine to  $4 \times 10^{-4}$  Pa, the film was etched at 60 sccm  $O_2$  flow ratio, 2 Pa pressure, 100 W input power, and 400 V automatic bias.

### Fabrication of the TENG

Two pieces of a 230  $\mu$ m thick Kapton film ( $4.5 \text{ cm} \times 4.5 \text{ cm}$  in size) were first cleaned with acetone, ethanol and deionized water for 15 minutes successively, and then the film was blow-dried. Then an Ag electrode was sputtered on the convex surface of each Kapton film. An oblique NW array was then fabricated on the concave surface of one piece of the Kapton film, the angle  $\alpha$  was  $30^\circ$ , and the etching time was 60 minutes. This film was subsequently immersed in a 2 M hydrochloric acid solution for 30 minutes to remove the metal or metal oxide particles on the surface of NWs and then washed with deionized water. The nylon solution was prepared by mixing formic acid and polyamide at a rate of 3 : 7 (w/w)

and then a thin film of the nylon solution was spin-coated on the concave surface of the other piece of the Kapton film with the speed of 2000 rpm for 30 s. The two pieces of films were then dried in an oven at 80 °C for 30 minutes and sealed together with the ONWAs facing the nylon film. The maximum distance between the two electrodes of the arch-shaped OTENG is about 15 mm. The VTENG and STENG have the same fabrication process as OTENG, except that the Kapton film with oblique NWs is replaced by a Kapton film with vertical NWs and a smooth Kapton film without treatment, respectively.

## Acknowledgements

We sincerely appreciate the financial support from NSFC (no. 51322203), the Fok Ying Tung education foundation (no. 131044), PCSIRT (no. IRT1251), and the “thousands talents” program for pioneer researcher and his innovation team, China and the Fundamental Research Funds for the Central Universities (no. lzujbky-2014-m02, no. lzujbky-2013-k04, lzujbky-2013-34, lzujbky-2013-230).

## Notes and references

- 1 R. J. Tseng, J. X. Huang, J. Ouyang, R. B. Kaner and Y. Yang, *Nano Lett.*, 2005, **5**, 1077.
- 2 M. Law, L. E. Greene, J. C. Johnson, R. Saykally and P. D. Yang, *Nat. Mater.*, 2005, **4**, 455.
- 3 J. A. Merlo and C. D. Frisbie, *J. Phys. Chem. B*, 2004, **108**, 19169.
- 4 Y. Chen and Y. Luo, *Adv. Mater.*, 2009, **21**, 2040.
- 5 K. S. Shin, T. Y. Kim, G. C. Yoon, M. K. Gupta, S. K. Kim, W. Seung, H. Kim, S. Kim, S. Kim and S. W. Kim, *Adv. Mater.*, 2014, **26**, 5619.
- 6 K. Wang, J. Huang and Z. Wei, *J. Phys. Chem. C*, 2010, **114**, 8062.
- 7 H. D. Tran, D. Li and R. B. Kaner, *Adv. Mater.*, 2009, **21**, 1487.
- 8 A. K. Wanekaya, Y. Lei, E. Bekyarova, W. Chen, R. Haddon, A. Mulchandani and N. V. Myung, *Electroanalysis*, 2006, **18**, 1047.
- 9 L. Liang, J. Liu, C. F. Windisch, G. J. Exarhos and Y. H. Lin, *Angew. Chem., Int. Ed.*, 2002, **41**, 3665.
- 10 H. Sato, D. Yagyu, S. Ito and S. Shoji, *Sens. Actuators, A*, 2006, **128**, 183.
- 11 Y. Zheng, X. Gao and L. Jiang, *Soft Matter*, 2007, **3**, 178.
- 12 W. Wu, L. Cheng, S. Bai, Z. L. Wang and Y. Qin, *Adv. Mater.*, 2012, **24**, 817.
- 13 H. E. Jeong, J. K. Lee, H. N. Kim, S. H. Moon and K. Y. Suh, *Proc. Natl. Acad. Sci. U. S. A.*, 2009, **106**, 5639.
- 14 L. Cheng, W. Dou, S. Bai, W. Wu, Q. Xu and Y. Qin, *Sci. Adv. Mater.*, 2013, **5**, 1179.
- 15 A. K. Khandpur, S. Forster, F. S. Bates, I. W. Hamley, A. J. Ryan, W. Bras, K. Almdal and K. Mortensen, *Macromolecules*, 1995, **28**, 8796.
- 16 H. Fang, W. Wu, J. Song and Z. L. Wang, *J. Phys. Chem. C*, 2009, **113**, 16571.
- 17 E. Wohlfart, J. P. Fernandez-Blazquez, E. Knoche, A. Bello, E. Perez, E. Arzt and A. del Campo, *Macromolecules*, 2010, **43**, 9908.
- 18 Y. N. Xia and G. M. Whitesides, *Annu. Rev. Mater. Sci.*, 1998, **28**, 153.
- 19 J. L. Wilbur, A. Kumar, H. A. Biebuyck, E. Kim and G. M. Whitesides, *Nanotechnology*, 1996, **7**, 452.
- 20 Y. N. Xia, E. Kim and G. M. Whitesides, *Chem. Mater.*, 1996, **8**, 1558.
- 21 L. J. Guo, *Adv. Mater.*, 2007, **19**, 495.
- 22 C. Liu, K. Hayashi and K. Toko, *Macromolecules*, 2011, **44**, 2212.
- 23 S. Y. Chou, P. R. Krauss, W. Zhang, L. J. Guo and L. Zhuang, *J. Vac. Sci. Technol., B*, 1997, **15**, 2897.
- 24 S. Y. Chou, P. R. Krauss and P. J. Renstrom, *J. Vac. Sci. Technol., B*, 1996, **14**, 4129.
- 25 C. M. Stafford, B. D. Vogt, C. Harrison, D. Julthongpiput and R. Huang, *Macromolecules*, 2006, **39**, 5095.
- 26 C. Beuret, G. A. Racine, J. Gobet, R. Luthier and N. F. de Rooij, *presented at Proceedings of the IEEE Workshop on Micro Electro Mechanical Systems*, 1994.
- 27 S. Pursel, M. W. Horn, M. C. Demirel and A. Lakhtakia, *Polymer*, 2005, **46**, 9544.
- 28 M. C. Demirel, S. Boduroglu, M. Cetinkaya and A. Lakhtakia, *Langmuir*, 2007, **23**, 5861.
- 29 J. R. Morber, X. Wang, J. Liu, R. L. Snyder and Z. L. Wang, *Adv. Mater.*, 2009, **21**, 2072.
- 30 B. O. Cho, S. W. Hwang, J. H. Ryu and S. H. Moon, *Rev. Sci. Instrum.*, 1999, **70**, 2458.
- 31 G. Zhu, C. Pan, W. Guo, C. Y. Chen, Y. Zhou, R. Yu and Z. L. Wang, *Nano Lett.*, 2012, **12**, 4960.
- 32 F. R. Fan, L. Lin, G. Zhu, W. Wu, R. Zhang and Z. L. Wang, *Nano Lett.*, 2012, **12**, 3109.
- 33 N. Vu and R. Yang, *Nano Energy*, 2013, **2**, 604.
- 34 Y. Yang, H. Zhang and Z. L. Wang, *Adv. Funct. Mater.*, 2014, **24**, 3745.
- 35 P. Bai, G. Zhu, Z. H. Lin, Q. Jing, J. Chen, G. Zhang, J. Ma and Z. L. Wang, *Acs Nano*, 2013, **7**, 3713.
- 36 K. Y. Lee, J. Chun, J. H. Lee, K. N. Kim, N. R. Kang, J. Y. Kim, M. H. Kim, K. S. Shin, M. K. Gupta, J. M. Baik and S. W. Kim, *Adv. Mater.*, 2014, **26**, 5037.
- 37 F. R. Fan, Z. Q. Tian and Z. L. Wang, *Nano Energy*, 2012, **1**, 328.
- 38 G. S. P. Castle, *J. Electrostat.*, 1997, **40–41**, 13.